**Advanced Research in Conservation Science**

**Journal homepage:** https://arcs.journals.ekb.eg

**DOI: 10.21608/arcs.2024.336172.1054**

# A Concise Look into Contact Angle Measurements in Heritage Characterization

**Mina Magdy***

*National Museum of Egyptian Civilization, 17611 Cairo, Egypt*

## HIGHLIGHTS

- Contact angle measurements are vital for evaluating the wetting characteristics of heritage materials.
- Enhance understanding of material behavior in response to environmental challenges.
- Combine contact angle data with surface chemistry for comprehensive insights.

## GRAPHICAL ABSTRACT

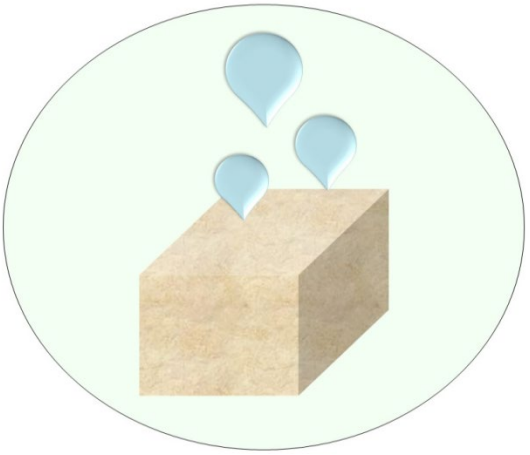

## ARTICLE INFO

**Article History:**
**Received: 13/11/2024**
**Accepted: 28/12/2024**
**Available Online: 28/12/2024**

**KEYWORDS:** Surface analysis, heritage characterization, wetting, contact angle measurement, surface chemistry.

## ABSTRACT

This article provides a body of knowledge on contact angle measurements and their role in heritage preservation. The contact angle method is an essential tool for evaluating the wetting characteristics of heritage materials, including stone, wood, textiles, and ceramics. The chemical composition and surface properties of heritage objects significantly influence their wetting behavior. The contact angle measurements offer insights into the hydrophobicity or hydro-philicity of materials and enhance our understanding of material behavior in response to environmental challenges. The effectiveness of conservation treatments often relies on the interaction between treatment agents and the substrate material.

*Corresponding Author,
E-mail: minamagdy_2000@yahoo.com

By correlating contact angle results with material composition, conservators can develop more effective preservation strategies tailored to specific materials. This approach ultimately strengthens the resilience of heritage objects against deterioration and loss over time. Contact angle measurements should be conducted in conjunction with surface structure and chemical composition analyses, as they do not provide a comprehensive description of surface properties.

## 1. Introduction

Cultural heritage conveys information about social and cultural backgrounds, serving as a bridge between contemporary society and the past, which is crucial for studying human civilization. Degradation phenomena are increasingly prominent in the field of cultural heritage [1]. Remedial conservation and preventive conservation are two distinct approaches to the long-term preservation of cultural heritage. Remedial conservation focuses on treating objects that have already suffered damage or deterioration. In contrast, preventive conservation encompasses a proactive strategy aimed at preventing future damage and ensuring the longevity of cultural heritage items [2].

Water is one of the dominant factors in weathering processes, acting as a catalyst for the degradation of heritage materials [3-6]. Common deterioration patterns include color change, fracturing, and swelling, which ultimately result in material loss [2]. Furthermore, the presence of water facilitates the growth of algae, fungi, lichens, and bacteria, leading to microbiological degradation [7]. The protection of archaeological objects from water is one of the main challenges for the conservation of cultural heritage because water is a major cause of material degradation, which may be chemical, physical or mechanical.

Water can originate from various sources, including rain, condensation due to relative humidity, or capillary rise from the soil. The protection process requires a thorough analysis of these water sources and pathways to effectively control water run-off. However, this can be difficult or insufficient in heritage artifacts due to various constraints. Therefore, a combined approach of chemical and physical protection is often essential to mitigate this issue [8].

Wettability (hydrophilicity/hydrophobicity) is a critical factor in the conservation of cultural heritage materials. Wettability and capillarity are interconnected phenomena that significantly influence how water interacts with the surfaces of archaeological objects.

Soluble salts present in porous materials can dissolve in water and migrate through capillary action. When water evaporates, these salts crystallize within the material, causing internal pressure that can lead to cracking or flaking [9,10]. For instance, the small contact angle of water droplets on murals indicates strong capillary activity involving both water and soluble salts, particularly in the ground layer.

Therefore, understanding wettability and capillarity is essential for conservation efforts, as managing moisture levels through controlled environments can help mitigate damage caused by excessive capillary action [11]. The chemical composition and surface properties of heritage objects further influence their wetting behavior. The presence of molecules (functional groups) on a material's surface can significantly alter its interaction with fluids [12,13]. Surface contamination significantly affects the

physico-mechanical properties of porous materials, necessitating consolidation treatments to restore material strength and maintain continuity in its physical and mechanical characteristics [14,15]. For surface protection strategies, protective consolidants have been employed in conservation to stabilize objects [16]. For instance, materials used for the consolidation of stones must impart hydrophobicity without blocking the stone's microstructure, thereby allowing the masonry to breathe and reduce salt efflorescence [17].

The consolidants used in conservation treatments require a thorough understanding of the object's properties [5]. A variety of protective materials have been developed to preserve the integrity of cultural heritage items and slow down the degradation process. These materials must fulfill several specific requirements, including transparency, chemical inertness, mechanical and physical durability, impermeability, solvent and acid resistance, good friction and anti-wear properties, strong adhesion, aesthetic appeal, reversibility, and long-term stability [1].

Since most alteration processes are driven by water, protective coatings should be designed to reduce the surface wettability of heritage objects. Therefore, there is an increased interest in the fabrication of super-hydrophobic and self-cleaning surfaces [7,18]. A defined protocol for coating applications includes the assessment of the conservation status of the object, creation of artificial specimens, testing of new coating products on standard objects, and validation of the durability and removability of protective coatings on ancient artifacts [19].

Analytical techniques provide potential for testing the performance of new conservation materials. Contact angle measurement is a widely used tool for characterizing surface properties and understanding liquid-solid interactions [20].Water contact angle (WCA) measurements can be applied in heritage characterization to assess how environmental conditions affect archaeological sites or museum collections, study the properties of materials used in restorations or reconstructions, and evaluate the impact of conservation treatments on artifacts [21,22]. Contact angle measurements do not alter the sample integrity, making them suitable for sensitive cultural heritage materials. However, a limitation of this method is that they cannot provide information about bulk properties or internal structures beyond surface interactions.

## 2. A guide to contact angle measurements

This section explores the scientific principle behind contact angle measurements. There are numerous arguments regarding wetting mechanisms and the manipulation of wetting behavior [20,23]. However, this article aims to clarify the fundamental surface concepts that underpin physical measurements. The wetting process is a phenomenon of solid surfaces that results from the adhesive forces between a solid surface and a liquid drop, as well as the cohesive forces within the liquid drop (Fig.1.) [24]. Strong cohesive forces among the liquid molecules result in higher contact angles, while strong adhesive forces between the liquid molecules and the solid surface lead to lower contact angles. Contact angle is one of the physical parameters to quantify the wettability of solid surfaces [25]. The contact angle measurement is defined as the angle formed at the interface between a liquid droplet and a solid surface, providing insights into the surface energy and hydrophobicity/hydrophilicity of materials. Geometrically, it is defined as the angle formed by a liquid at the three-phase

boundary point where a solid, liquid, and gas intersect [23]. Young's Equation describes the balance at the three-phase contact.

Surfaces with identical chemical compositions but differing roughness exhibit varying contact angles. When the contact angle is less than 90°, the solid surface is classified as hydrophilic, indicating high wettability. Conversely, when the water contact angle exceeds 90°, the solid surface is classified as hydrophobic, indicating low wettability. If the water contact angle is significantly smaller than 10° or greater than 150°, the solid surface is referred to as superhydrophilic or superhydrophobic, respectively [22,25]. Upon adsorption, the liquid contracts its surface area to maintain the lowest surface free energy.The intermolecular force responsible for this contraction is known as surface tension, which determines the shape of liquid droplets [23]. The droplet shape that minimizes Gibbs free energy corresponds to an equilibrium state where the balance between cohesive and adhesive forces is achieved. Therefore, the contact angle is inherently linked to the intrinsic properties of the surface [26].

Wettability on a flat and chemically homogeneous surface is described by Young's equation: $\mathrm{Cos}\theta = (\gamma_{sv} - \gamma_{sl})/\gamma_{lv}$ [27]. In this equation, $\theta$ represents the static contact angle, while $\gamma_{sv}$, $\gamma_{sl}$, and $\gamma_{lv}$ denote the solid-vapor, solid-liquid, and liquid-vapor interfacial energies, respectively.

Young's equation is strictly applicable only to completely smooth surfaces. However, many materials exhibit roughness and heterogeneity on their surfaces. Surface roughness contributes to the generation of hysteresis, where microscopic variations in slope on the surface create barriers that pin the motion of the contact line, thus altering the macroscopic contact angles. Therefore, interpreting angle data using Young's Equation can be misleading, as the equation does not take surface topography into account. The Wenzel and Cassie-Baxter models are commonly used theories that aim to describe the homogeneous and heterogeneous wettability of rough substrates, respectively [23,24]. When a droplet rests on rough substrates where water molecules do not fill the grooves, wettability can be explained by the Wenzel model, which is represented by: $\gamma_{lv}\cdot\mathrm{Cos}\theta_W = r\cdot(\gamma_{sv} - \gamma_{sl})$.

Here, $\mathrm{Cos}\theta_W$ denotes the contact angle of the droplet in the Wenzel state, and r is the roughness factor defined as the ratio of the actual surface area to the apparent surface area of the substrate. Combining the Wenzel's equation with Young's Equation yields: $\mathrm{Cos}\theta_W = r\cdot\mathrm{Cos}\theta$ [28-30].

In contrast, in the Cassie-Baxter model, water molecules completely fill the grooves of a rough surface and do not penetrate into the liquid phase. For chemically heterogeneous surfaces, the chemical composition varies at different locations, and the apparent contact angle may differ from one point on the solid surface to another [24]. The relationship is given by: $\mathrm{Cos}\theta_{CB} = f_1\cdot\mathrm{Cos}\theta_1 + f_2\cdot\mathrm{Cos}\theta_2$ [29-31].

In this equation, $\mathrm{Cos}\theta_{CB}$ denotes the contact angle of the droplet in the Cassie-Baxter state, accounting for the contributions from different surface areas. Here, $f_1$ represents the surface fraction of material 1 with intrinsic contact angle $\theta_1$, while $f_2$ represents the surface fraction of material 2 with intrinsic contact angle $\theta_2$. In many cases, particularly when dealing with superhydrophobic surfaces ($\theta_2 = 180°$, $\mathrm{Cos}\theta_2 = -1$), the equation can be re-written as

follows: $Cos\theta_{CB} = f_1 \cdot Cos\theta_1 - f_2$ [30]. The measurement of contact angle hysteresis is often recommended as a method to assess the quality of the substrate surface [23]. An ideal surface is smooth, chemically homogeneous, and free of hysteresis. In this case, the local energy profile at each site would be identical, possessing a single minimum point that represents the only stable thermodynamic state attainable by the system. Surface non-uniformity results in multiple Gibbs energy minima and the formation of different actual contact angles ($ACCA_s$) at each site along the droplet's periphery, which do not accurately represent the overall surface features.

The Wenzel and Cassie-Baxter equations are based on hypothetical surfaces with average properties that represent the original surface features. Replacing a real surface with an equivalent ideal surface characterized by a single Gibbs energy minimum allows for the determination of the most stable energy state [24].

In this context, the use of a larger droplet would minimize the effects of surface heterogeneity. The higher internal energy of a larger droplet would aid its movement beyond the energy state barrier toward the global energy minimum, which aligns with the averaging approach used in the Wenzel and Cassie-Baxter wetting models (Fig. 2) [26]. Furthermore, while discrepancies frequently occur between the calculated Wenzel and Cassie angles and the experimentally observed angles, these differences can be reconciled by modifying classic roughness factors with correction factors that account for the geometry of the rough contact line [20]. Computational simulations (e.g., molecular dynamics simulations) have validated that both Cassie-Baxter and Wenzel models predict contact angle measurements well on rough surfaces, making them valuable for understanding wetting phenomena in various applications [29].

A droplet of liquid in the millimeter range is placed on a surface using a dosing unit. The use of small droplets helps prevent deformation of water droplets caused by gravity [32]. Ultrapure water is commonly used to avoid the presence of ions and organic molecules that can alter surface tension and wettability characteristics, potentially leading to misleading results in contact angle measurements [33,34]. For instance, the presence of salts can change the surface tension and wetting properties of water, allowing it to spread more easily over a surface and thereby reducing the contact angle [35]. Ultrapure water is typically utilized as a probing liquid in archaeological contexts to simulate the effects of humidity on heritage objects. When comparing the wetting phenomena of different surfaces, it is essential to measure contact angles with water droplets of identical volume [25].The drop dispensing process should be gentle, minimizing disturbance to the sessile drop caused by the micro-syringe needle and drop impact, in order to maintain data consistency [20]. The droplet is observed with a high-resolution camera to capture images from the moment it adheres to the surface. The entire single droplet must be located within the region of interest. The measurement of the contact angle depends on the optical acquisition of the droplet profile [26]. The quality measurement variables include camera resolution, image magnification, light levels, depth of field, and contrast with the background. The choice of the image analysis algorithm is crucial because different algorithms can give different values of contact angles [36].

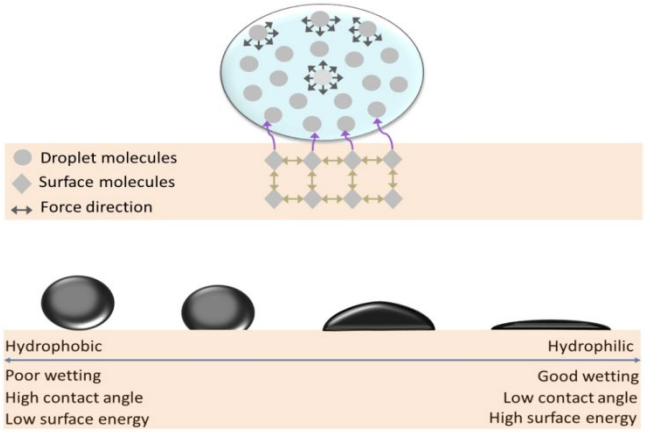


**Fig.1. Schematic representation illustrating how the interaction between droplet and surface molecules influences wetting behavior and contact angle.**

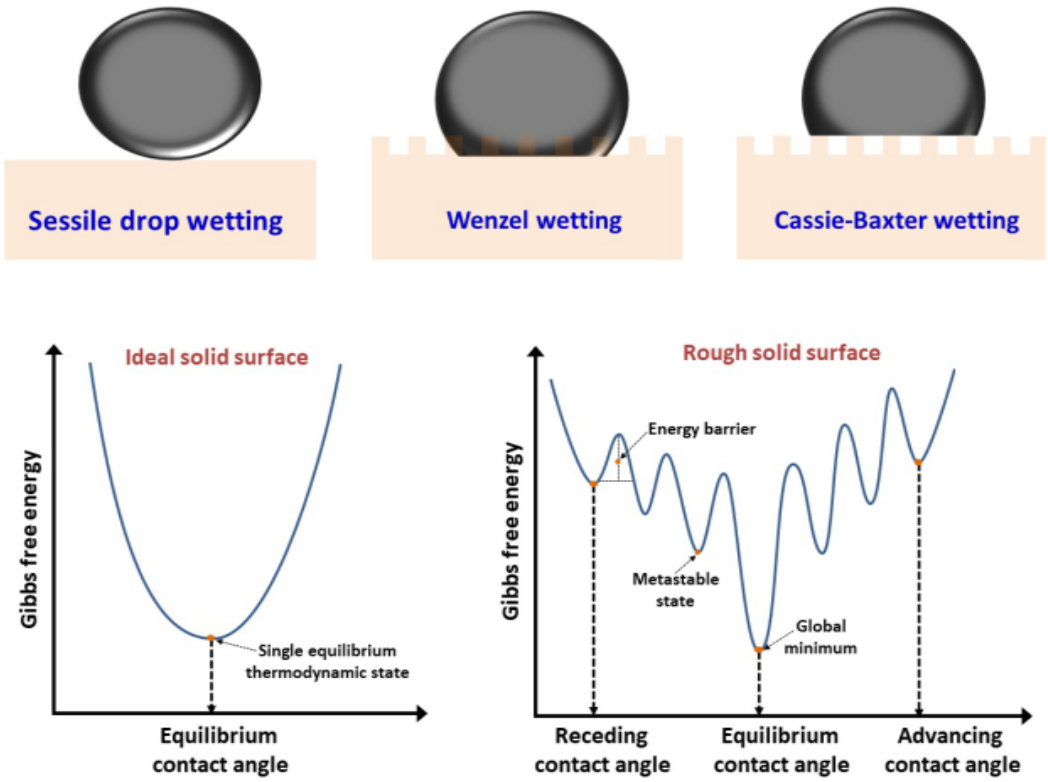


**Fig.2. Schematic representation of droplet configurations in the sessile drop, Wenzel, and Cassie-Baxter wetting models, along with Gibbs energy diagrams for both ideal and rough solid surfaces.**

The software calculates the contact angle after defining the baseline and the droplet shape. Several well-developed conventional methods are available for measuring contact angles, including confocal microscopy, environmental scanning electron microscopy, and atomic force microscopy [25,26]. The baseline of the measurement is the horizontal line representing the solid surface onto which the droplet is deposited. The contact angle is formed at the point where this baseline intersects the edge of the droplet. By using the gradient of the tangent at the droplet edge that meets the baseline, the contact angle between them can be calculated using trigonometric functions. One of the main challenges in contact angle measurements is the absence of reference standards for measurement methods. Different techniques can produce varying contact angle values, even when the same liquid is applied to a specific surface [20]. This underscores the importance of careful consideration when interpreting contact angle data across different studies. Contact angle measurements are mainly performed using static and dynamic methods. Static contact angles (sessile drop method) are measured when the three boundary phases are static. A droplet of liquid is placed on the surface, and the angle is measured once equilibrium is reached. The static contact angle can be defined by fitting with various modes, such as ellipse, circle, tangent, polynomial, and Laplace-Young fitting [20,25]. In contrast, dynamic contact angles are measured when the three boundary phases are in motion as the droplet advances or recedes from the surface. The difference between the advancing and receding contact angles is referred to as hysteresis, which quantifies the variability in wetting behavior as a droplet moves across a surface [37]. A larger hysteresis indicates a greater difference between the advancing and receding contact angles of a liquid droplet on that surface.

Contact angle hysteresis (CAH) is influenced by several factors, including surface topology, surface roughness, chemical heterogeneity, and the surface energy of the material [38]. The wettability of solid surfaces is governed by the surface topology along the contact line of the droplet [39]. Measuring contact angles on non-planar surfaces introduces complexities related to droplet positioning and interpretation. Rough surfaces can entrap air pockets beneath a droplet, hindering its ability to spread uniformly and decreasing the contact area with the surface [40,41].Additionally, variations in chemical composition and geometrical microstructure across a surface can create regions with different wettability, causing droplets to behave differently depending on their movement direction. For instance, the presence of hydrophobic groups on a surface can reduce its surface energy and enhance its water-repellent properties [42].

Also, the balance between cohesive and adhesive forces is directly related to surface energy, which determines how a liquid droplet interacts with a surface, influencing wettability and contact angle. A high surface energy (indicating stronger adhesive forces) typically corresponds to better wettability, while low surface energy can lead to poor wettability (indicating stronger cohesive forces). Surface energy is influenced by the material's chemical composition and surface structure [43]. The Gibbs free energy of a system, a specific thermodynamic potential, can be used to calculate the Gibbs free energy barrier associated with advancing and receding contact angles. This barrier

represents the energy required to change the wettability state of a surface. The Gibbs free energy barrier is defined as the difference in Gibbs free energy between a local minimum (representing a stable wetting state) and an adjacent maximum (representing an unstable or transitional state) in the direction of three-phase line motion (i.e., advancing or receding) [44]. A lower energy barrier corresponds to a lower advancing angle and greater spreading across the surface, while a higher barrier indicates higher receding angles and poorer wettability [45,46]. Thus, the energy barrier is crucial for predicting wetting behavior.

The accuracy of contact angle measurements is highly dependent on surface cleanliness; therefore, surfaces should be thoroughly cleaned before conducting measurements. Measurements should be repeated at different locations of the same sample or across different specimens of the same type that have undergone identical cleaning procedures. Generally, the average and standard deviation of the valid contact angles are recorded [38]. The entire apparatus should be placed on a vibration-free table to ensure that drop formation is not affected by vibrational noise from the surrounding environment, thereby avoiding any additional kinetic energy [20,38].

Controlling consistent environmental conditions, such as in climate-controlled laboratories, is crucial for obtaining reproducible and accurate contact angle data [47]. Temperature variations can alter the viscosity and surface tension of liquids and affect the properties of the solid surface, leading to changes in contact angle values [20]. Humidity influences the adsorption of water vapor onto surfaces, modifying surface energy and consequently affecting wettability. Variations in air pressure can further impact droplet shape and its interaction with surfaces. Therefore, maintaining stable temperature, humidity, and air pressure is essential to minimize the impact of environmental variability on contact angle measurements. Furthermore, contact angle readings can be influenced by factors such as porosity, surfactant-like contamination, and the shape and size of surface particles [30].

## 3. Application aspects of contact angle measurements

This section discusses the importance of contact angle measurements within the characterization framework in an archaeological context, offering insights into surface properties. Apostolopoulou *et al.* investigated consolidation treatments for marble sugaring, which exhibited significant granular disaggregation. Two different materials were utilized, both with and without the addition of sodium stearate. The first material was a suspension of calcium hydroxide ($Ca(OH)_2$) combined with 6% by weight of calcium carbonate ($CaCO_3$), referred to as reinforced lime.

The second material was a novel nano-dispersion of calcium hydroxide ($Ca(OH)_2$) in ethyl alcohol ($C_2H_5OH$) at a concentration of 15 g/L. The reinforced lime treatments (RL, RL_30, RL_90 based on the addition of mg/L sodium stearate) and the nano-dispersion consolidation treatments (NL, NL_30, NL_90 based on the addition of mg/L sodium stearate) were conducted over a period of two weeks. The treated specimens were then placed in a vessel with 75% relative humidity (T: 20 ± 1 °C) for two months (in a supersaturated solution of $NH_4Cl$) to ensure complete carbonation of the consolidation materials and conversion of calcium hydroxide to calcite.

Static contact angle measurements were performed on the marble specimens before and after applying the consolidation materials. Before treatment, the untreated specimens exhibited a static contact angle lower than 90°. After consolidation, the contact angle increased, reaching values well above 90° in all cases, indicating that all consolidated surfaces could be considered hydrophobic.

All treated specimens showed contact angle values exceeding 120°, which was reported as the highest value achieved through purely chemical processes on smooth surfaces. These results indicated that all applied treatments modified the static contact angle values of the surface and might confer protective effects on the marble surface. Notably, the standard deviation of static contact angle measurements for untreated specimens was significantly higher than that of the same specimens after consolidation treatments; this was attributed to the greater homogeneity of the consolidated surfaces. The higher static contact angles were achieved with the NL treatments. In both cases, reinforced lime and nanolime, the addition of sodium stearate appeared to slightly increase the static contact angle. This might be linked to a certain degree of hydrophobicity in the precipitated calcite crystals formed in the presence of sodium stearate on the consolidated surface. Increasing the quantity of sodium stearate beyond 30 mg/L did not seem to influence this characteristic significantly, especially when considering the standard deviation.

The highest static contact angle values were observed in specimens treated with the nanodispersion of calcium hydroxide combined with sodium stearate. The treatment involving the nanodispersion of calcium hydroxide (15 g/L) with an addition of 90 mg/L sodium stearate (NL_90) appeared to be optimal for consolidating pentelic marble surfaces exhibiting granular disaggregation, since it yielded one of the highest static contact angles [48].

Uc-Fernández *et al.* studied the anti-corrosive properties of superhydrophobic hexadecyltrimethoxysilane (HDTMS) functionalized MCM-41 silica particles (MCM-41-HDTMS) within the sol-gel matrix of ORMOSIL methyltriethoxysilane (MTES) for metal protection, using commercial copper (Cu) and carbon steel (Fe) sheets as substrates.

The contact angle measurements were performed using the sessile drop technique. Uncoated samples exhibited low water contact angles, remaining hydrophilic, with measured angles of 79° and 75° for the copper and iron specimens, respectively. The MTES gel contributed to the hydrophobicity of the materials, resulting in contact angles of 126° for Fe-MTES and 145° for Cu-MTES. However, when MCM-41-HDTMS was incorporated into the coating systems, water contact angles of 137° and 155° were achieved for Fe-MTES-HDTMS and Cu-MTES-HDTMS, respectively. The addition of MCM-41-HDTMS to the MTES matrix induced an increase in the contact angle by approximately 10 degrees, along with an enhancement in its dispersive component due to the substantial deposition of long carbon chains from HDTMS over the high surface area of the MCM-41 particles.

The increase in water contact angle values for samples containing MCM-41-HDTMS might be attributed to the generation of dual-scale roughness; nanoscale roughness was imparted by MCM-41-HDTMS materials, which was interconnected with MTES gel at the microscale. This created a heterogeneous surface that aligned with the Cassie-Baxter

wettability model for rough and heterogeneous surfaces, allowing large air bubbles to be trapped between the surface and liquid, thereby enhancing water repellency.

Additionally, the sprocketed structure of long carbon chain functionalization on the surface of MCM-41-HDTMS could alter the coating systems due to changes in surface energy associated with these nanoparticles. The incorporation of MCM-41-HDTMS nanoparticles improved hydrophobicity and consequently enhanced the anti-corrosive properties of coatings synthesized with MTES ORMOSIL deposited on both copper and carbon steel substrates [49].

Li *et al.* conducted a consolidation study of waterlogged archaeological wood from the bottom plate of the Zhangwan No. 3 shipwreck in Shuangjie Town, China. The wood blocks were consolidated using polydimethylsiloxane (PDMS) or cross-linked PDMS chains with reversibly N-coordinated boroxines ($NCB_s$) to produce PDMS-NCB, as well as polyethylene glycol (PEG1000), which had an average molecular weight of 1000 g/mol. Time-dependent water contact angles were measured for the wood (W), W-PDMS-NCB, W-PDMS, and W-PEG1000 samples in an environment with 58% relative humidity (RH). The water contact angle on the W sample was 80.1°, indicating that the surface of the wood sample was hydrophilic. Moreover, time-dependent contact angle measurements showed that the water droplet on the W sample was quickly absorbed, causing the water contact angle to decrease to 0° within 5 s due to the porous structure of the wood sample. Therefore, the hydrophilic nature of hemicellulose and cellulose, along with the porous structure of the wood sample, contributed to its ability to easily absorb moisture and exhibited unsatisfactory humidity stability. In contrast, the water droplet on the W-PDMS-NCB sample was barely absorbed, and its water contact angle remained nearly constant over 120 s.

The water contact angle on the W-PDMS-NCB sample was approximately 118.3°, demonstrating its hydrophobic surface. The hydrophobic PDMS chains and cross-linked structure of the in-situ formed PDMS-NCB polymers acted as dense barrier layers on both the surface and inside of the wood, effectively preventing water droplets from penetrating the W-PDMS-NCB sample, thereby endowing it with excellent humidity stability. Meanwhile, the W-PDMS sample exhibited a hydrophobic surface with a water contact angle of approximately 127.6°.

However, water droplets on the W-PDMS sample were noticeably absorbed, resulting in a decrease in the water contact angle to around 100.9° within 120 s. In addition, the initial water contact angle of the W-PEG1000 sample was only 18.0°, significantly lower than that of the wood sample. Water droplets on the W-PEG1000 sample were rapidly absorbed, causing the water contact angle to decrease to 4.5° within 15 s. All of these results confirmed that the W-PEG1000 sample exhibited the poorest humidity stability due to the high hydrophilicity of PEG1000. The in-situ construction of hydrophobic and cross-linked PDMS-NCB conservation materials endowed the W-PDMS-NCB sample with excellent humidity stability, surpassing that of the wood, W-PDMS, and W-PEG1000 samples [50].

Badea *et al.* discussed the effect of halloysite nanotube (HNT) dispersions on vegetable-tanned leather from a historical bookbinding at the Vaslui County Museum.

The three dispersions were referred to as HNT-beeswax (beeswax/1-chlorobutane), HNT-PEG (polyethylene glycol), and HNT-BNUTO (a hydroalcoholic solution of urea and sodium chloride). The treatments were applied through total immersion of the leather samples for 10 min, followed by air drying.

To determine the dynamics of contact angle changes over time, the shape of the liquid droplet was recorded by a camera from the moment the drop was placed on the sample (at t = 0 s) until 120 s, with intervals of 3 s. For each sample, three measurements were taken from different spots, and the average of these values was reported as the contact angle. The initial contact angle (t = 1 s) and final contact angle (t = 120 s) were used for analysis. The contact angle of untreated leather decreased at a constant rate until the water droplet was fully absorbed (approximately 1 min). For both HNT-PEG and HNT-BNUTO treatments, the water droplet was completely absorbed in 20 s. In contrast, for the HNT-beeswax treatment, a two-rate absorption process was observed: a steeper absorption rate during the first 2 min, followed by a slower rate up to 5 min. The contact angle measurements indicated that a hydrophobic effect was generated by the HNT-beeswax treatment, while the other treatments resulted in increased water absorption by the leather [51].

Wang *et al.* developed a polyvinyl alcohol–ethylene glycol (PVA-EG) hydrogel for the removal of animal glue from book surfaces based on fluorescent-labeling evaluation. The hydrogel samples were prepared by mixing PVA at various concentrations (6%, 8%, 10%, and 12%) with EG in a mass ratio of 4:6. The surface wettability of the hydrogel samples was tested on filter paper coated with europium nitrate-fluorescent animal glue using a contact angle measuring instrument. The pure PVA sample exhibited a larger initial contact angle, which decreased slowly over time, indicating poor surface wettability and relatively weak water absorption capacity.

This behavior could be attributed to stronger hydrogen bonding between the pure PVA molecular chains, resulting in tighter molecular packing and less exposure of hydrophilic groups, thereby reducing interaction with water molecules. As the concentration of EG increased, the contact angle of the hydrogel gradually decreased, significantly improving wettability. Notably, in the 10% and 12% PVA-EG samples, water droplets spread considerably within 0.1 s and were almost fully absorbed after 0.4 s, with the contact angle approaching 0. This indicated that the introduction of EG markedly enhanced the hydrophilicity and water absorption capacity of the PVA hydrogel.

EG molecules formed new hydrogen bonds with PVA molecular chains, increasing the polarity of the hydrogel and the density of hydrophilic groups. This structural change increased the surface free energy of the hydrogel, facilitating interactions with water molecules and accelerating water absorption and penetration. The results indicated that the PVA-EG hydrogel could effectively remove glue layers within a relatively short-time frame [52].

## 4. Conclusions

The physical properties (e.g., porosity and texture) and chemical properties (e.g., composition and structure) of heritage materials affect their durability and vulnerability to degradation. Wettability describes how a liquid spreads over or

penetrates a solid surface. High water wettability on archaeological surfaces can lead to increased moisture absorption, which may promote biological growth and chemical deterioration. Contact angle measurements offer valuable insights into the hydrophobic or hydrophilic nature of materials, enabling the assessment of their susceptibility to moisture-related damage.

Contact angle data can be integrated into predictive models that simulate the behavior of cultural heritage materials in different environmental conditions. However, contact angle analyses have certain limitations. Variation in surface conditions, such as roughness or contamination, can impact the accuracy of measurements. Advances in scientific technology and computational modeling could further refine these analyses and enhance their precision. The methods for measuring contact angles can aid in developing proactive conservation strategies that are tailored to specific materials and environmental conditions.

**References**


1. J. Xu, Y. Jiang, T. Zhang, Y. Dai, D. Yang, F. Qiu, Z. Yu, and P. Yang, "Fabrication of UV-curable waterborne fluorinated polyurethane-acrylate and its application for simulated iron cultural relic protection," *Journal of Coatings Technology and Research*, Vol. 15, No. 3, 2018, pp. 535–541.
2. M. Ben Chobba, M.L. Weththimuni, M. Messaoud, C. Urzi, and M. Licchelli, "Recent advances in the application of metal oxide nanomaterials for the conservation of stone artefacts, ecotoxicological impact and preventive measures," *Coatings*, Vol. 14, No. 2, 2024, pp. 203.
3. L. De Ferri, P.P. Lottici, A. Lorenzi, A. Montenero, and E. Salvioli-Mariani, "Study of silica nanoparticles–polysiloxane hydrophobic treatments for stone-based monument protection," *Journal of Cultural Heritage*, Vol. 12, No. 4, 2011, pp. 356–363.
4. A. Tsigarida, E. Tsampali, A.A. Konstantinidis, and M. Stefanidou, "On the use of confocal microscopy for calculating the surface microroughness and the respective hydrophobic properties of marble specimens," *Journal of Building Engineering,* Vol. 33, 2021, pp. 101876.
5. J. Xu, Y. Jiang, T. Zhang, Y. Dai, D. Yang, F. Qiu, Z. Yu, and P. Yang, "Fabrication of UV-curable waterborne fluorinated polyurethane-acrylate and its application for simulated iron cultural relic protection," *Journal of Coatings Technology and Research*, Vol. 15, No. 3, 2018, pp. 535–541.
6. M. Ben Chobba, M.L. Weththimuni, M. Messaoud, C. Urzi, and M. Licchelli, "Recent advances in the application of metal oxide nanomaterials for the conservation of stone artefacts, ecotoxicological impact and preventive measures," *Coatings*, Vol. 14, No. 2, 2024, pp. 203.
7. L. De Ferri, P.P. Lottici, A. Lorenzi, A. Montenero, and E. Salvioli-Mariani, "Study of silica nanoparticles–polysiloxane hydrophobic treatments for stone-based monument protection," *Journal of Cultural Heritage*, Vol. 12, No. 4, 2011, pp. 356–363.
8. A. Tsigarida, E. Tsampali, A.A. Konstantinidis, and M. Stefanidou, "On the use of confocal microscopy for calculating the surface microroughness and the respective hydrophobic

properties of marble specimens," *Journal of Building Engineering,* Vol. 33, 2021, pp. 101876.

9. C.D. Vacchiano, L. Incarnato, P. Scarfato, D. Acierno, "Conservation of tuff-stone with polymeric resins," *Construction and Building Materials*, Vol. 22, No. 5, 2008, pp. 855–865.
10. B.S.M. Mazen, B.M. Ismail, H.R.R. Ali, and M. Ali, "Damage caused by black inks to the chemical properties of archaeological papyrus – analytical study," *Pigment and Resin Technology*, Vol. 52, No. 1, 2023, pp. 73–81.
11. Y. Zhang, L. Vespignani, M.G. Balzano, L. Bellandi, M. Camaiti, N. Lubin-Germain, and A. Salvini, "Low fluorinated oligoamides for use as wood protective coating," *Coatings*, Vol. 12, No. 7, 2022, pp. 927.S. Andreotti, E. Franzoni, M.D. Esposti, P. Fabbri, "Poly (hydroxyalkanoate)s- based hydrophobic coatings for the protection of stone in cultural heritage," *Materials*, Vol. 11, No. 1, 2018, pp. 165.
12. C. Lisci, C. Galhano, J. Simão, V. Pires, F. Sitzia, and J. Mirão, "Hydrophobic coatings' efficiency and limestones' resistance to salt crystallization," *Sustainability*, Vol. 16, No. 2, 2024, pp. 816.
13. S. Pasquale and A.M. Gueli. "Effect of water in color changes of historical paintings," *Color Research and Application*, Vol. 46, No. 6, 2021, pp. 1265–1275.
14. Q. Xia and W. Dong. "Research on the reinforcement and inhibition of water–salt activity in mural ground layers by superhydrophobic $SiO_2$ particles," *Crystals*, Vol. 13, No. 10, 2023, pp. 1522.
15. K. Buczkowska, "Hydrophobic protection for building materials," in *Superhydrophobic Coating - Recent Advances in Theory and Applications*, J. Ou, Ed. Rijeka: In-TechOpen, 2023, pp.1-25.
16. F. Duan, Y. Zhu, Y. Lu, X. Wang, and A. Wang, "Preparation of pre-wetted underwater superoleophobic porous material from green water-based foam for oil–water separation," *Journal of Materials Science*, Vol. 57, 2022, pp. 9172–9186.
17. O. Rudic, D. Rajnovic, D. Cjepa, S. Vucetic, and J. Ranogajec, "Investigation of the durability of porous mineral substrates with newly designed $TiO_2$-LDH coating," *Ceramics International*, Vol. 41, No. 8, 2015, pp. 9779-9792.
18. J.M. Tulliani, A. Formia, and M. Sangermano, "Organic-inorganic material for the consolidation of plaster," *Journal of Cultural Heritage*, Vol. 12, No. 4, 2011, pp. 364–371.
19. G. Aleksić, T. Cigula, M. Vukoje, and I.K. Itrić, "Bilayer coating composed of starch and methyl cellulose-nanoscale $TiO_2$ for the protection of historic paper from UV," *Coatings*, Vol. 13, No. 5, 2023, pp. 899.
20. R.A. Walker, K. Wilson, A.F. Lee, J. Woodford, V.H. Grassian, J. Baltrusaitis, G. Rubasinghege, G. Cibin, and A. Dent, "Preservation of York Minster historic limestone by hydrophobic surface coatings," *Scientific Reports*, Vol. 2, 2012, pp. 880.
21. L. Guo, L. Wang, X. Zhao,M. Peng,"Non-whitening superhydrophobic coating for heritage protection,"Colloids and Surfaces A: Physicochemical and

Engineering Aspects, Vol. 676, 2023, pp. 132294.
22. A. Artesani, F. Di Turo, M. Zucchelli, and A. Traviglia, "Recent advances in protective coatings for cultural heritage–an overview," *Coatings*, Vol. 10, No. 3, 2020, pp. 217.
23. K.Y. Law and H. Zhao, *Surface Wetting: Characterization, Contact Angle, and Fundamentals.* Cham: Springer, 2016.
24. G. Wang, Y. Chai, Y. Li, H. Luo, B. Zhang, and J. Zhu, "Sandstone protection by using nanocomposite coating of silica," *Applied Surface Science*, Vol. 615, 2023, pp. 156193.
25. F.M. Helmi and Y.K. Hefni, "Nanocomposites for the protection of granitic obelisks at Tanis, Egypt," *Mediterranean Archaeology and Archaeometry*, Vol. 16, 2016, pp. 87–96.
26. Y. Yuan and T.R. Lee, "Contact angle and wetting properties," in *Surface Science Techniques*, G. Bracco and B. Holst, Eds. Berlin: Springer, 2013, pp.3–34.
27. V. Dutschk and A. Marmur, "The contact angle as an analytical tool," in *Colloid and Interface Chemistry for Nanotechnology*, P. Kralchevsky, R. Miller, and F. Ravera, Eds. Boca Raton: CRC Press, 2014, pp.255–270.
28. T. Zhao and L. Jiang, "Contact angle measurement of natural materials," *Colloids and Surfaces B: Biointerfaces*, Vol. 161, 2018, pp. 324–330.
29. C.H. Kung, P.K. Sow, B. Zahiri, and W. Mérida, "Assessment and interpretation of surface wettability based on sessile droplet contact angle measurement: challenges and opportunities," *Advanced Materials Interfaces*, Vol. 6, No. 18, 2019, pp. 1900839.
30. T. Young, "An essay on the cohesion of fluids," *Philosophical Transactions of the Royal Society of London*, Vol. 95, 1805, pp. 65–87.
31. R.N. Wenzel, "Resistance of solid surfaces to wetting by water," *Industrial and Engineering Chemistry*, Vol. 28, No. 8, 1936, pp. 988–994.
32. H. Yaghoubi and M. Forouta, "Molecular investigation of the wettability of rough surfaces using molecular dynamics simulation," *Physical Chemistry Chemical Physics*, Vol. 20, No. 34, 2018, pp. 22308–22319.
33. T.T. Chau, W.J. Bruckard, P.T. Koh, and A.V. Nguyen, "A review of factors that affect contact angle and implications for flotation practice," *Advances in Colloid and Interface Science*, Vol. 150, No. 2, 2009, pp. 106–115.
34. A.B.D. Cassie and S. Baxter, "Wettability of porous surfaces," *Transactions of the Faraday Society*, Vol. 40, 1944, pp. 546–551.
35. U.A. Ivanovich, P.T. Nickolayevna, and K.A. Viktorovich, "The effect of the loss of superhydrophobic surface properties on biofouling and flow around shipbuilding's steel plates," *Ocean Engineering*, Vol. 214, 2020, pp. 107801.
36. M. Poitevin, Y. Shakalisava, S. Miserere, G. Peltre, J.L. Viovy, and S. Descroix, "Evaluation of microchip material and surface treatment options for IEF of allergenic milk proteins on microchips," *Electrophoresis*, Vol. 30, No. 24, 2009, pp. 4256–4263.

37. F. Artusio, F. Fumagalli, J. Bañuls-Ciscar, G. Ceccone, R. Pisano, "General and adaptive synthesis protocol for high-quality organo-silane self-assembled monolayers as tunable surface chemistry platforms for biochemical-applications, Bio inter phases, Vol. 15, No.4, 2020, pp. 041005.
38. N.S. Muhammed, B. Haq and D.A. Al Shehri, "Hydrogen storage in depleted gas reservoirs using nitrogen cushion gas: a contact angle and surface tension study," *International Journal of Hydrogen Energy*, Vol. 48, No. 98, 2023, pp. 38782–38807.
39. M. Vuckovac, M. Latikka, K. Liu, T. Huhtamäki, and R.H. Ras, "Uncertainties in contact angle goniometry," *Soft Matter*, Vol. 15, No. 35, 2019, pp. 7089–7096.
40. W.A. Zisman, "Surface energetics of wetting spreading and adhesion," *Journal of Paint Technology*, Vol. 44, No. 564, 1972, pp. 42–57.
41. D. M. Fopp-Spori, "Surface characterization by contact angle measurements," in *Biofouling Methods*, S. Dobretsov, J.C. Thomason, and D.N. Williams, Eds. Chichester: Wiley-Blackwell, 2014, pp–318–325.
42. M.A. Khandoker and K. Golovin, "Statistical heuristic wettability analysis of randomly textured surfaces," *Langmuir*, Vol. 36, No. 47, 2020, pp. 14361–14371.
43. S. Rabbani, E. Bakhshandeh, R. Jafari, and G. Momen, "Superhydrophobic and icephobic polyurethane coatings: fundamentals, progress, challenges and opportunities," *Progress in Organic Coatings*, Vol. 165, 2022, pp. 106715.
44. L.A. Carrascosa, R. Zarzuela, M. Botana-Galvín, F.J. Botana, and M.J. Mosquera, "Achieving super-hydrophobic surfaces with tunable roughness on building materials via nanosecond laser texturing of silane/ siloxane coatings," *Journal of Building Engineering*, Vol. 58, 2022, pp. 104979.
45. R. Jafari and M. Farzaneh, "Development a simple method to create the super-hydrophobic composite coatings, "Journal of Composite Materials, Vol. 47, No. 25, 2013, pp. 3125–3129.
46. C. Zhao, S. Zhang, Q. Fan, W. Wang, J. Zhao, and S. Yi, "Understanding wetting behaviors on rough PTFE surfaces towards n-octane/water mixture separation by molecular dynamics simulation," *Materials Today Communications*, Vol. 40, 2024, pp. 109935.
47. S. Moradi, P. Englezos, and S.G. Hatzikiriakos,"Contact angle hysteresis: surface morphology effects," *Colloid and Polymer Science*, Vol. 291, 2013, pp. 317–328.
48. L. Liu, S. Wang, X. Zeng, P. Pi, and X. Wen, "Dropwise-condensation by nano-engineered surfaces:design, mechanism, and enhancing strategies. *Advanced Materials Interfaces*, Vol. 8, No. 24, 2021, pp. 2101603.
49. J.B. Boreyko, R.R. Hansen, K.R. Murphy, S. Nath, S.T. Retterer, and C.P. Collier, "Controlling condensation and frost growth with chemical micro-patterns," *Scientific Reports*, Vol. 6, 2016, pp. 19131.
50. M. Grüßer, D.G. Waugh, J. Lawrence, N. Langer, and D. Scholz, "On the droplet size and application of wettability analysis for the development

of ink and printing substrates," *Langmuir*, Vol. 35, No. 38, 2019, pp. 12356–12365.

51. M. Apostolopoulou, E. Drakopoulou, M. Karoglou, and A. Bakolas, "Consolidation treatments for marble sugaring: reinforced lime versus nanolime," *Materials and Structures*, Vol. 54, 2021, pp. 195.
52. E. Uc-Fernández, J. González-Sánchez, A. Ávila-Ortega, Y. Pérez-Padilla, J.M. Cervantes-Uc, J. Reyes-Trujeque, W.A. and Talavera-Pech, "Anticorrosive properties of a superhydrophobic coating based on an ORMOSIL enhanced with MCM-41-HDTMS nanoparticles for metals protection," *Journal of Coatings Technology and Research*, Vol. 20, 2023, pp. 347–357.
53. S. Li, Y. Zeng, L. Zhou, N. Feng, C. Li, L., Sheng, Y. Li, and J. Sun, "Consolidation of waterlogged archaeological woods by reversibly cross-linked polymers," *Journal of Archaeological Science: Reports*, Vol. 57, 2024, pp. 104675.
54. E. Badea, C. Carşote, E. Hadîmbu, C. Șendrea, and M.C. Lupaș, "The effect of halloysite nanotubes dispersions on vegetable-tanned leather thermal stability," *Heritage Science*, Vol. 7, 2019, pp. 68.
55. J. Wang, Y. Xu, C. Tian, Y. Yu, and C. Zou, "Application of polyvinyl alcohol–ethylene glycol hydrogel technology for removing animal glue in book restoration based on fluorescent labeling evaluation," *Nanomaterials*, Vol. 14, 2024, pp. 1878.